Research Square

Preprints are preliminary reports that have not undergone peer review.
They should not be considered conclusive, used to inform clinical practice,
or referenced by the media as validated information.

Potential distribution of Ixodes persulcatus (Ixodidae) in Mongolia

Munkhjargal Dorjravdan
National Center for Communicable Diseases
Uyanga Baasandavga
National Center for Zoonotic Diseases
Batbayar Ochirbat
National Center for Communicable Diseases
RK Raghavan
raghavanrk@missouri.edu

University of Missouri

Article

Keywords: Ixodes persulcatus, ecological niche modeling, MaxEnt, tick-borne encephalitis, Mongolia, climate suitability

Posted Date: September 1st, 2026

DOI: https://doi.org/10.21203/rs.3.rs-10657989/v1

License: This work is licensed under a Creative Commons Attribution 4.0 International License.
Read Full License

Additional Declarations: No competing interests reported.

Abstract

The taiga tick (*Ixodes persulcatus*) is a major vector of tick-borne pathogens in Mongolia and throughout the Palearctic region. The current potential spatial distribution of this species in Mongolia is not clearly understood. We compiled occurrence records from across Eurasia and Mongolia and applied a rigorous MaxEnt modeling framework incorporating extensive parameter tuning and model selection. Median ensemble predictions indicated a broad zone of climatic suitability extending from eastern Fennoscandia and across Russia to Mongolia, northeastern China, and the Korean Peninsula. Within Mongolia, northern, central, and northeastern regions exhibited the highest suitability. These findings provide the high-resolution prediction of *I. persulcatus* distribution in Mongolia and offer a spatial foundation for targeted tick surveillance and tick-borne disease prevention strategies.

Introduction

Ticks are among the most important arthropod vectors of disease affecting humans and domestic animals worldwide[1,2]. *Ixodes persulcatus*, commonly known as the taiga tick, is a principal vector of multiple zoonotic pathogens across the Palearctic region and represents a growing public health concern in Mongolia[3,4]. The burden associated with *I. persulcatus*–borne infections has increased steadily over recent decades, reflecting both ecological change and expanding human exposure[5]. This species is implicated in the transmission of pathogens responsible for significant morbidity and mortality, including *Borrelia burgdorferi* (Lyme disease), tick-borne encephalitis virus (TBEV), *Anaplasma phagocytophilum*, and *Borrelia miyamotoi*[3,6]. Tick-borne encephalitis is among the most consequential vector-borne viral diseases in Eurasia, with thousands of cases reported annually[7]. Unlike *Ixodes ricinus*, *I. persulcatus* is associated with both European and Far Eastern subtypes of TBEV, the latter characterized by substantially higher case fatality rates[7–9]. Recent detection of *Candidatus Rickettsia tarasevichiae* in *I. persulcatus* ticks from northern Mongolia further underscores the emerging public health risks linked to this vector[10,11].

Mongolia shares extensive borders with Russia and China and supports a large nomadic pastoral population that depends on livestock rearing. Livestock numbers in this region exceeded 57 million in 2024, and frequent close contact between herders, livestock, and wildlife creates favorable conditions for the transmission of tick-borne pathogens[4,12]. Over the past two decades, both the number of fatal tick-borne disease cases and their geographic extent have increased in Mongolia, with *I. persulcatus* identified as the primary vector[8,9,13]. Further, molecular surveillance studies have revealed high rates of pathogen co-infection in Mongolian *I. persulcatus* populations, with up to 40% of ticks carrying multiple pathogens simultaneously[14,15].

Climate change is increasingly recognized as a major driver of shifts in tick distributions[16]. Rising temperatures over the past three decades have been associated with earlier seasonal activity, prolonged transmission periods, and establishment of *I. persulcatus* in previously unsuitable regions of

northeastern Asia[5,17,18]. These changes amplify human exposure risk and highlight the need for updated spatial predictions to guide adaptive surveillance strategies[19–21].

Understanding the spatial distribution of vector species is essential for effective disease prevention and control[22]. Tick distributions are constrained by habitat suitability, which is shaped by climatic and environmental conditions that influence development, survival, and population dynamics[23,24]. Species distribution modeling provides a powerful framework for predicting potential distributions based on environmental correlates of known occurrences[25,26]. Among available tools, the MaxEnt algorithm is widely used for tick habitat suitability modeling because of its strong performance with presence-only data and small sample sizes[20,21,27–31]. However, nationwide mapping of suitable habitat for *I. persulcatus* in Mongolia remains limited despite recent regional studies documenting changing patterns of TBE incidence and tick activity[9,32].

In this study, we calibrated ecological niche models using the broad Eurasian distribution of *I. persulcatus* and transferred these models to Mongolia to estimate its potential distribution. By integrating extensive occurrence data with a rigorous model selection procedure, we aimed to provide the high-resolution, statistically robust prediction of climatic suitability for *I. persulcatus* in Mongolia, thereby supporting improved surveillance and control of tick-borne diseases.

Results

Occurrence data and preprocessing

The Global Biodiversity Information Facility (GBIF) dataset yielded 587 occurrence records spanning Finland, Sweden, Ukraine, Latvia, Estonia, Belarus, Lithuania, Russia, Kazakhstan, Kyrgyzstan, China, Japan, and Mongolia, reflecting the broad Palearctic distribution of *I. persulcatus* (Fig. 1). An additional 20 records were obtained from the National Center for Zoonotic Diseases (NCZD), resulting in 607 records initially. One record lacking geographic coordinates was removed, leaving 606 unique records. After cleaning and removal of duplicates and minor spatial mismatches, 406 unique records remained, consistent with recommended data preprocessing workflows for ecological niche modeling[28,33].

Spatial thinning reduced the datasets to 261 occurrences (10 km), 199 occurrences (20 km), and 164 occurrences (30 km), effectively minimizing spatial clustering while retaining adequate sample sizes for robust model calibration[33,34]. For each thinned dataset, 495 candidate models were evaluated. Three models met all selection criteria for the 10 km dataset, and five models were retained for each of the 20 km and 30 km datasets. Selected models had regularization multipliers ranging from 0.1 to 1.0 and included linear, quadratic, and product feature classes, indicating that moderately flexible response functions best captured the species–environment relationships[28,35].

Median ensemble predictions revealed a broad zone of climatic suitability extending from eastern Fennoscandia and across Russia to Mongolia, northeastern China, and the Korean Peninsula (Fig. 2).

Within Mongolia, northern, central, and northeastern regions exhibited the highest predicted suitability (Fig. 3), aligning closely with known TBE-endemic areas and regions where *I. persulcatus* has been previously reported[8,9]. At the Eurasian scale, uncertainty of predicted suitable areas was concentrated in Afghanistan, Tajikistan, Kyrgyzstan, Turkey, Georgia, and most notably in China (Fig. 4). In Mongolia, uncertainty was localized in Bulgan and Arkhangai provinces, although the value of the range remained low (Fig. 5).

Across selected models, habitat suitability was driven primarily by nonlinear responses and interactions among principal components.

Model selection and performance

Selected models had regularization multipliers ranging from 0.1 to 1.0 and included linear, quadratic, and product feature classes. All retained models were statistically significant (partial ROC, $p < 0.05$) and satisfied omission rate thresholds (≤ 5%). Ensemble agreement was highest across boreal and forest-steppe zones.

Predicted distribution patterns

The quadratic term of PC3 emerged as the strongest predictor, indicating a unimodal response along this environmental gradient. Interactions between PC1 and PC2 consistently ranked second in importance, highlighting multidimensional niche structure and reinforcing the importance of considering interaction effects in ecological niche modeling[28,35] (Supplementary Table S1). Response curves for all PCs exhibited unimodal shapes, with maximum suitability at intermediate values (Fig. 6), a pattern commonly observed in ectothermic arthropods constrained by physiological tolerances[23,33].

Principal component analysis (PCA) was used to summarize the correlation structure among the bioclimatic variables prior to modelling. The first four principle components (PC1-PC4) together explained 95.4% of the total climatic variance. PC1 and PC2 accounted for the largest proportion of variation (66.2%), indicating that a limited number of climatic gradients capture most of the variability in the environmental space. PC3 and PC4 captured additional variability related to precipitation intensity during the wet season and temperature variability, respectively. The loadings of the original bioclimatic variables on each axis are allowing evaluation of the contribution of individual climatic variables to the PCA axes (Supplementary Table S2 and Supplementary Table S3). The distribution of occurrence records along the first two PCA axes shows how tick occurrence points are positioned relative to the major climatic gradients represented by the PCA components (Supplementary Fig. S1). Climatic variables associated with temperature extremes and seasonality exhibited the strongest loadings on PC1, whereas precipitation-related variables contributed more strongly to PC2. Most occurrence records clustered within a relatively narrow region of the environmental space, indicating that the species occupies a restricted climatic niche primarily associated with cold continental climates[24,36].

Discussion

Using a rigorously calibrated MaxEnt modeling framework and a comprehensive, multi-source occurrence dataset, this study provides the first high-resolution prediction of the potential distribution of *I. persulcatus* in Mongolia. Ensemble projections revealed a continuous band of climatically suitable habitat extending from eastern Fennoscandia and the Baltic region across boreal and temperate Russia into Mongolia, northeastern China, and the Korean Peninsula. This spatial pattern closely mirrors the well-documented Palearctic range of the taiga tick and reinforces its ecological affinity for cool, humid, and seasonally variable environments characteristic of boreal and forest-steppe biomes[3,4,18,20].

Within Mongolia, predicted suitability was highest in northern, central, and northeastern provinces, including Hentii, Dornod, Suhbaatar, Uvurhangai, Huvsgul, Bulgan, Arhangai, Selenge, Orhon, Tuv, and Darhan-Uul. These regions are dominated by taiga and forest-steppe ecosystems with relatively cool summers, adequate summer precipitation, and stable humidity conditions that favor off-host survival, successful molting, and sustained questing activity[2,36,37]. The emergence of northeastern Mongolia as a high-suitability zone is particularly noteworthy, as this region forms an ecological corridor connecting suitable habitats in southern Siberia with those in northeastern China. Such transboundary continuity suggests that population connectivity and gene flow may facilitate the spread of both ticks and tick-borne pathogens across national borders, underscoring the importance of coordinated international surveillance and control efforts[3,17,18,20].

Previous studies have modeled the potential distribution of *I. persulcatus* at a global scale[3]. For instance, Wang et al. used MaxEnt to identify key climatic predictors and predicted suitable habitats globally, including parts of Mongolia[3]. However, global-scale models often rely on relatively sparse occurrence records from Mongolia and therefore may not fully capture local ecological conditions. By using a regionally calibrated modeling framework and updated occurrence data, our results provide more detailed and spatially refined assessment of climatically suitable habitats for *I. persulcatus* in Mongolia. This regional approach improves the understanding of the species' ecological niche within Mongolia and helps identify areas where surveillance and tick-borne disease monitoring may be particularly important. Precipitation-related variables exerted a dominant influence on predicted suitability, with declines observed under both insufficient and excessive rainfall regimes. Adequate summer precipitation is critical for maintaining high relative humidity within forest litter and understory vegetation, which in turn supports egg viability, larval survival, and prolonged host-seeking behavior[2,37]. These findings are consistent with experimental and field-based studies demonstrating that desiccation stress is a primary limiting factor for ixodid ticks and that moisture availability often constrains their southern and western range margins[19,21,24]. Conversely, excessive precipitation may disrupt microhabitat stability, increase fungal growth, and reduce host availability, thereby lowering habitat suitability[25,37].

Temperature-related gradients also played a key role in shaping the modeled niche of *I. persulcatus*. The unimodal responses observed across principal components suggest that both extreme cold and

excessive warmth impose physiological constraints on development and survival[23,33]. Cold-season severity, continentality, and temperature seasonality emerged as major contributors, reflecting the species' adaptation to environments with long winters and pronounced seasonal contrasts[3,36]. However, warming trends associated with climate change are likely to shift these optimal conditions northward and to higher elevations, potentially enabling further expansion into previously unsuitable areas of central and eastern Mongolia. Such dynamics are consistent with recent empirical evidence documenting earlier seasonal activity, extended questing periods, and elevational range shifts in *I. persulcatus* and other temperate tick species[5,17,18,21].

However, variation among the three model projections (Fig. 4) suggests the presence of uncertainty in predicted suitable areas at the Eurasian scale. The moderate uncertainty concentrated in Afghanistan, Tajikistan, Kyrgyzstan, Turkey, Georgia, and most notably in central and southern part of China. These regions are characterized by strong environmental gradients and complex topography, which can challenge niche-based modeling approaches and lead to increased variability among model outputs[25,38]. Furthermore, sparse and uneven occurrence data in several of these areas likely amplified model sensitivity and contributed to greater prediction uncertainty[21,25,38]. In contrast, predicted suitable areas within Mongolia exhibited relatively low uncertainty, indicating strong agreement among selected models and suggesting robust suitability estimates. Overall, regions with low uncertainty represent more reliable suitability predictions, whereas high-uncertainty areas should be interpreted cautiously and prioritized for enhanced field surveillance to improve future modeling efforts.

The public health implications of these findings are substantial. *I. persulcatus* is the principal vector of tick-borne encephalitis virus in Mongolia, and reported incidence of TBE is highest in provinces that closely overlap with the predicted high-suitability zones identified here, including Selenge, Bulgan, Darhan-Uul, and Orhon[8,9,39]. Human exposure risk is strongly shaped by occupational and recreational activities prevalent in forested regions, such as herding, forestry, pine nut and wild plant collection, wood gathering, and mining[4,40]. In addition to TBEV, *I. persulcatus* in Mongolia transmits a diverse assemblage of pathogens of veterinary and public health importance, including *Babesia* spp., *Anaplasma phagocytophilum*, *Borrelia burgdorferi*, *Borrelia miyamotoi*, *Candidatus Neoehrlichia mikurensis*, and *Candidatus Rickettsia tarasevichiae*[6,10,14,41]. The high frequency of pathogen co-infections documented in Mongolian tick populations further amplifies the risk of complex clinical presentations and diagnostic challenges, particularly in resource-limited rural settings[14,42].*Candidatus Rickettsia tarasevichiae*[6,10,14,41]. The high frequency of pathogen co-infections documented in Mongolian tick populations further amplifies the risk of complex clinical presentations and diagnostic challenges, particularly in resource-limited rural settings[14,42]. From a One Health perspective, the convergence of suitable tick habitat, dense livestock populations, and nomadic pastoral practices creates a landscape of heightened zoonotic risk. Livestock serve not only as blood-meal hosts that sustain tick populations but also as potential reservoirs or sentinels for several tick-borne pathogens[4,40]. Economic impacts linked to tick infestations and tick-borne infections in livestock—including reduced milk and meat production, anemia, abortion,

and mortality—compound the public health burden and highlight the need for integrated surveillance strategies that jointly monitor ticks, wildlife, livestock, and human populations[20,43–45].

The habitat suitability maps generated in this study provide a practical foundation for risk-based allocation of public health and veterinary resources. Prioritizing surveillance in areas where high human activity overlaps with predicted high suitability for *I. persulcatus* could improve early detection of emerging foci and enhance the efficiency of prevention efforts[20,22]. In Mongolia, many high-risk regions are sparsely populated and have limited healthcare infrastructure, increasing the likelihood of underdiagnosis and underreporting of tick-borne diseases[4,8]. Establishing sentinel surveillance sites, conducting seroprevalence studies in humans and animals, and integrating tick monitoring into existing public health programs would help validate model predictions and refine estimates of true disease burden[11,20,39].

Several limitations should be acknowledged. First, the MaxEnt approach is inherently correlative and does not explicitly model the physiological mechanisms governing tick survival, reproduction, or dispersal[26,27]. Second, our models rely primarily on broad-scale climatic variables and do not incorporate finer-scale determinants of microhabitat suitability, such as vegetation structure, land use, soil moisture, and host community composition[20,24,28]. As a result, the predictions represent climatic suitability rather than realized tick density or direct human exposure risk. Third, the occurrence data used here, although extensive, are subject to spatial sampling biases and temporal heterogeneity that may influence model outcomes[33,34]. Incorporating bias-correction techniques, high-resolution land cover data, and mechanistic components in future modeling efforts would likely improve predictive accuracy[21,28,46].

Finally, climatic suitability alone does not equate to disease risk. Pathogen prevalence in tick populations, human behavior patterns, vaccination coverage against TBE, and access to healthcare services all modulate observed disease outcomes[7,22,39]. Integrating these epidemiological and socio-behavioral factors with predicted tick distributions would enable development of more comprehensive risk assessment frameworks for tick-borne diseases in Mongolia[20,25]. Despite these limitations, our findings provide a critical baseline for understanding the spatial ecology of *I. persulcatus* and for guiding evidence-based interventions aimed at mitigating the growing burden of tick-borne diseases across the region.

This study provides robust, high-resolution predictions of climatically suitable habitat for *Ixodes persulcatus* across Eurasia, with a particular focus on Mongolia, using a rigorously calibrated MaxEnt modeling framework and comprehensive model selection procedures. The results confirm the species' strong association with boreal and temperate forest zones extending from eastern Fennoscandia to the Russian Far East and identify northern, central, and northeastern Mongolia as regions of high potential suitability. These areas overlap closely with known foci of tick-borne encephalitis and regions where *I. persulcatus* and multiple tick-borne pathogens have been previously documented, underscoring the public health relevance of the predicted patterns.

By filling a critical knowledge gap in tick ecology and distribution in Mongolia, this work offers an essential baseline for future entomological surveys, disease surveillance programs, and risk-based public health and veterinary interventions. The habitat suitability maps generated here provide a practical foundation for prioritizing surveillance in high-risk regions, optimizing resource allocation, and supporting transboundary monitoring efforts with neighboring countries. Integrating these predictions with epidemiological, ecological, land-use, and socio-behavioral data will be key to improving prevention and control of tick-borne diseases in Mongolia and across the broader Palearctic region, particularly in the context of ongoing climate change.

Methods

Tick occurrence data

Occurrence records for *I. persulcatus* were obtained from the GBIF and the NCZD in Mongolia. The GBIF dataset comprised records collected between 1946 and 2025 across Eurasia[47] whereas the NCZD dataset included records from Mongolia collected between 2017 and 2019. All records included geographic coordinates in decimal degrees. Data were screened to remove duplicates and records with erroneous or imprecise locations, following standard best practices for species distribution modeling[28,33].

To define the area accessible to the species (M), we delineated regions within 2.25° (~ 250 km) of known occurrence points using the Grinnell package in R. This accessible area represents the region plausibly reached by the species through dispersal over relevant time scales and constitutes the appropriate geographic extent for model calibration and evaluation[48,49].

To reduce spatial autocorrelation and minimize sampling bias, we applied spatial thinning using three distance thresholds (10 km, 20 km, and 30 km) with the spThin package in R[34]. The thinning procedure was repeated three times for each threshold, retaining randomly selected representative occurrence locations and generating three independent occurrence datasets, a strategy shown to improve model robustness and reduce overfitting[33,46].

Environmental data

Bioclimatic variables were obtained from WorldClim at a spatial resolution of 2.5 arc-minute, a resolution commonly used in continental-scale ecological niche modeling[20,21,25]. Maximum temperature, minimum temperature, and precipitation variables were included. Variables known to exhibit spatial artifacts (mean temperature of wettest quarter - bio8, mean temperature of driest quarter - bio9, precipitation of warmest quarter - bio18, precipitation of coldest quarter - bio19) were excluded to avoid spurious model behavior[50]. Fifteen bioclimatic variables were retained to capture climatic heterogeneity within the accessible area. To reduce multicollinearity and improve model interpretability, we conducted principal component analysis (PCA) on the selected variables[28,35]. The first four principal components (PC1–

PC4), explaining 95% of the total variance, were retained for model calibration. Univariate response curves were generated to examine relationships between environmental gradients and predicted suitability.

Ecological niche modeling

Ecological niche models were developed using the MaxEnt algorithm implemented in the dismo package in R. Given the sensitivity of MaxEnt to parameterization and feature selection, we conducted a detailed model selection procedure using the kuenm package[27,51]. We evaluated all combinations of regularization multiplier values (0.1, 0.25, 0.5, 0.75, 1–5), feature class combinations (linear, quadratic, product, threshold, hinge), and the selected predictor set. In total, 495 candidate models were calibrated for each occurrence dataset.

Models were evaluated and selected based on three criteria: (1) statistical significance using partial ROC tests, which provide a robust alternative to conventional AUC for presence-only data[26]; (2) predictive performance measured by omission rates at a 5% threshold[35]; and (3) model complexity assessed using the Akaike Information Criterion corrected for small sample sizes (AICc), based on 10-fold cross-validation[35,52]. Final models were required to be statistically significant, have omission rates ≤ 5%, and fall within 2 AICc units of the best-performing model. Selected models were transferred to the broader Eurasian region and to Mongolia. Median ensemble predictions from the retained models were used as the basis for interpretation, following best practices for reducing uncertainty in model projections[20,21,25]. Uncertainty in predicted suitable areas was assessed using the pixel-wise range (maximum-minimum) across selected model outputs.

Declarations

Competing interests

The authors declare no competing interests.

Author Contribution

R.K.R., M.D. designed the study; performed experiments and wrote the manuscripts and prepared figures; U.B. provided occurrence data; O.B. wrote the manuscript. All authors reviewed the manuscript.

Acknowledgement

This study was partially funded by the Taylor Geospatial Institute (TGI). The authors are grateful to the grant funding, and TGI did not have any role in the conceptualization, design, methods, or findings

reported in this study.

Data Availability

Data used in conducting this study are available for researchers upon request to the corresponding author for reasonable use in research.

References

1. Madison-Antenucci, S., Kramer, L. D., Gebhardt, L. L. & Kauffman, E. Emerging tick-borne diseases. *Clin. Microbiol. Rev.* **33** https://doi.org/10.1128/CMR.00083-18 (2020).
2. Estrada-Peña, A. Ticks as vectors: taxonomy, biology and ecology. *Rev. Sci. Tech.* **34**, 53–65. https://doi.org/10.20506/rst.34.1.2345 (2015).
3. Wang, S. S. et al. Geographical distribution of Ixodes persulcatus and associated pathogens: Analysis of integrated data from a China field survey and global published data. *One Health*. **16**, 100508. https://doi.org/10.1016/j.onehlt.2023.100508 (2023).
4. Černý, J., Buyannemekh, B., Needham, T., Gankhuyag, G. & Oyuntsetseg, D. Hard ticks and tick-borne pathogens in Mongolia—A review. *Ticks Tick. Borne Dis.* **10**, 101268. https://doi.org/10.1016/j.ttbdis.2019.101268 (2019).
5. Gray, J. S., Ogden, N. H. & Ticks Human Babesiosis and Climate Change. *Pathogens* **10**, 1430. https://doi.org/10.3390/pathogens10111430 (2021).
6. Karnath, C. et al. Detection of Babesia venatorum, Anaplasma phagocytophilum and Candidatus Neoehrlichia mikurensis in Ixodes persulcatus ticks from Mongolia. *Ticks Tick Borne Dis*. 7, 357–360 (2016). (2016). https://doi.org/10.1016/j.ttbdis.2015.12.007
7. Bogovic, P. & Strle, F. Tick-borne encephalitis: A review of epidemiology, clinical characteristics, and management. *World J. Clin. Cases*. **3**, 430–441. https://doi.org/10.12998/wjcc.v3.i5.430 (2015).
8. Baasandavga, U. et al. A case series of fatal meningoencephalitis in Mongolia: Epidemiological and molecular characteristics of tick-borne encephalitis virus. *West. Pac. Surveill Response J.* **10**, 1–7. https://doi.org/10.5365/WPSAR.2018.9.1.003 (2019).
9. Baasandavga, U. et al. Geographical distribution of tick-borne encephalitis and its vectors in Mongolia, 2005–2016. *Cent. Asian J. Med. Sci.* **3**, 250–258. https://doi.org/10.24079/CAJMS.2017.11.006 (2017).
10. Boldbaatar, B. et al. Distribution and molecular characteristics of rickettsiae found in ticks across Central Mongolia. *Parasites Vectors*. **10**, 61. https://doi.org/10.1186/s13071-017-1981-3 (2017).
11. von Fricken, M. E. et al. Estimated seroprevalence of Anaplasma spp. and spotted fever group Rickettsia exposure among herders and livestock in Mongolia. *Acta Trop.* **177**, 179–185. https://doi.org/10.1016/j.actatropica.2017.10.015 (2018).

12. National Statistics Office of Mongolia. News release. The total number of livestock. (2025). https://downloads.1212.mn/LIw4s_EFj0rbSK-PjdqG-Ml32-0z_2eJB-caGto_.pdf
13. Tserennorov, D. et al. TBE in Mongolia. Tick-borne encephalitis. (2023). https://tbenews.com/tbe/13-22-9/
14. Lagunova, E. K. et al. Co-infections with multiple pathogens in natural populations of *Ixodes persulcatus* ticks in Mongolia. *Parasites Vectors*. **15**, 253. https://doi.org/10.1186/s13071-022-05356-x (2022).
15. Tian, J. et al. Molecular surveillance reveals a potential hotspot of tick-borne disease in Yakeshi City, Inner Mongolia. *BMC Microbiol.* **23**, 110. https://doi.org/10.1186/s12866-023-03110-6 (2023).
16. Alkishe, A., Raghavan, R. K. & Peterson, A. T. Likely geographic distributional shifts among medically important tick species and tick-associated diseases under climate change in North America: a review. *Insects* **12**, 225. https://doi.org/10.3390/insects12030225 (2021).
17. Ma, R. et al. The current distribution of tick species in Inner Mongolia and inferring potential suitability areas for dominant tick species based on the MaxEnt model. *Parasites Vectors*. **16**, 286. https://doi.org/10.1186/s13071-023-05870-6 (2023).
18. Yang, X. et al. Mapping the potential distribution of major tick species in China. *Int. J. Environ. Res. Public. Health*. **17**, 1–15. https://doi.org/10.3390/ijerph17145145 (2020).
19. Gasmi, S. et al. Evidence for increasing densities and geographic ranges of tick species of public health significance. *PLoS ONE*. **13** https://doi.org/10.1371/journal.pone.0201924 (2018).
20. Raghavan, R. K., Townsend Peterson, A., Cobos, M. E., Ganta, R. & Foley, D. Current and future distribution of the Lone Star tick, Amblyomma americanum (L.) in North America. *PLoS One*. **14** https://doi.org/10.1371/journal.pone.0209082 (2019).
21. Raghavan, R. K. et al. Potential spatial distribution of the long-horned tick, Haemaphysalis longicornis in North America. *Sci. Rep.* **9**, 498. https://doi.org/10.1038/s41598-018-37205-2 (2019).
22. Eisen, R. J. & Eisen, L. Spatial modeling of human risk of exposure to vector-borne pathogens based on epidemiological versus arthropod vector data. *J. Med. Entomol.* **45**, 181–192. https://doi.org/10.1093/jmedent/45.2.181 (2008).
23. Estrada-Peña, A. Tick-borne pathogens, transmission rates and climate change. *Front. Biosci.* **14**, 2674–2687. https://doi.org/10.2741/3405 (2009).
24. Estrada-Peña, A., Ayllón, N. & de la Fuente, J. Impact of climate trends on tick-borne pathogen transmission. *Front. Physiol.* **3**, 64. https://doi.org/10.3389/fphys.2012.00064 (2012).
25. Elith, J. & Leathwick, J. R. Species distribution models: Ecological explanation and prediction across space and time. *Annu. Rev. Ecol. Evol. Syst.* **40**, 677–697. https://doi.org/10.1146/annurev.ecolsys.110308.120159 (2009).
26. Peterson, A. T. Uses and requirements of ecological niche models. *Ecol. Modell*. **190**, 231–259. https://doi.org/10.1016/j.ecolmodel.2005.03.026 (2006).

27. Phillips, S. B., Aneja, V. P., Kang, D. & Arya, S. P. Maximum entropy modeling of species geographic distributions. *Ecol. Modell*. **190**, 231–259. https://doi.org/10.1016/j.ecolmodel.2005.03.026 (2006).
28. Merow, C., Smith, M. J. & Silander, J. A. A practical guide to MaxEnt for modeling species' distributions: What it does, and why inputs and settings matter. *Ecography* **36**, 1058–1069. https://doi.org/10.1111/j.1600-0587.2013.07872.x (2013).
29. Raghavan, R. K. et al. Predicting the potential distribution of Amblyomma americanum (Acari: Ixodidae) infestation in New Zealand, using maximum entropy-based ecological niche modelling. *Exp. App Acarology*. **80**, 227–245. https://doi.org/10.1007/s10493-019-00460-7 (2016).
30. Boorgula, G. D. Y., Peterson, T., Foley, A., Ganta, D. H., Raghavan, R. K. & R. R. & Assessing the current and future potential geographic distribution of the American dog tick, Dermacentor variabilis (Say) (Acari: Ixodidae) in North America. *PLoS One*. **15**, e0237191. https://doi.org/10.1371/journal.pone.0237191 (2020).
31. Raghavan, R. K., Koestel, Z., Ierardi, R., Peterson, A. T. & Cobos, M. E. Climatic suitability of the eastern paralysis tick, Ixodes holocyclus, and its likely geographic distribution in the year 2050. *Sci. Rep.* **11** https://doi.org/10.1038/s41598-021-94793-2 (2021).
32. Cleary, N. G. et al. Detection of tick-borne encephalitis virus in Ixodes ticks collected near Ulaanbaatar, Mongolia. *Open. Forum Infect. Dis.* **6** https://doi.org/10.1093/ofid/ofaf673 (2025).
33. Wisz, M. S. et al. Effects of sample size on the performance of species distribution models. *Divers. Distrib.* **14**, 763–773. https://doi.org/10.1111/j.1472-4642.2008.00482.x (2008).
34. Aiello-Lammens, M. E. et al. An R package for spatial thinning of species occurrence records for use in ecological niche models. *Ecography* **38**, 541–545. https://doi.org/10.1111/ecog.01132 (2015).
35. Warren, D. L. & Seifert, S. N. Ecological niche modeling in Maxent: The importance of model complexity and the performance of model selection criteria. *Ecol. Appl.* **21**, 335–342. https://doi.org/10.1890/10-1171.1 (2011).
36. Bugmyrin, S. V. & Bespyatova, L. A. Seasonal activity of adult ticks Ixodes persulcatus (Acari, Ixodidae) in the north-west of the distribution area. *Animals* **13**, 3834. https://doi.org/10.3390/ani13243834 (2023).
37. Bugmyrin, S. V., Bespyatova, L. A. & Korotkov, Y. S. Long-term dynamics of Ixodes persulcatus (Acari: Ixodidae) abundance in the north–west of its range (Karelia, Russia). *Exp. Appl. Acarol*. **77**, 229–240. https://doi.org/10.1007/s10493-019-00342-y (2019).
38. Owens, H. L. et al. Constraints on interpretation of ecological niche models by limited environmental ranges on calibration areas. *Ecol. Model.* **236**, 10–18. https://doi.org/10.1016/j.ecolmodel.2013.04.01 (2013).
39. Ganbold, D. et al. Seroprevalence and risk factors of tick-borne encephalitis in Mongolia between 2016 and 2022. *Parasite Epidemiol. Control*. **22** https://doi.org/10.1016/j.parepi.2023.e00318 (2023).
40. Von Fricken, M. E. et al. Geographic Range of Lyme Borreliosis in Mongolia. *Vector-Borne Zoonotic Dis.* **19**, 658–661. https://doi.org/10.1089/vbz.2018.2421 (2019).

41. Otgonsuren, D. et al. Molecular survey of bovine Babesia species in Bactrian camels (Camelus bactrianus) in Mongolia. *Ticks Tick. Borne Dis.* **13**, 658–661. https://doi.org/10.1016/j.ttbdis.2021.101871 (2019).
42. Tian, D. et al. Distribution and diversity of ticks determined by environmental factors in Ningxia, China. *One Health*. **19** https://doi.org/10.1016/j.onehlt.2024.100897 (2024).
43. Jones, K. E. et al. Global trends in emerging infectious diseases. *Nature* **451**, 990–993. https://doi.org/10.1038/nature06536 (2008).
44. Enkhtaivan, B. et al. Molecular detection of Anaplasma ovis in small ruminants and ixodid ticks from Mongolia. *Parasitol. Int.* **69**, 47–53. https://doi.org/10.1016/j.parint.2018.11.004 (2019).
45. Stuen, S., Granquist, E. G. & Silaghi, C. Anaplasma phagocytophilum—A widespread multi-host pathogen with highly adaptive strategies. *Front. Cell. Infect. Microbiol.* **3**, 31. https://doi.org/10.3389/fcimb.2013.00031 (2013).
46. Kopsco, H. L., Smith, R. L. & Halsey, S. J. A scoping review of species distribution modeling methods for tick vectors. *Front. Ecol. Evol.* **10**, 893016. https://doi.org/10.3389/fevo.2022.893016 (2022).
47. GBIF.org. GBIF Occurrence Download. (30. June (2025).
48. Soberon, J. & Peterson, A. Interpretation of models of fundamental ecological niches and species' distributional areas. (2005). https://doi.org/10.17161/bi.v2i0.4
49. Machado-Stredel, F., Cobos, M. E. & Peterson, A. T. A simulation-based method for selecting calibration areas for ecological niche models and species distribution models. *Front. Biogeogr.* **13** https://doi.org/10.21425/F5FBG48814 (2021).
50. Escobar, L. E., Lira-Noriega, A. & Medina-Vogel, G. Townsend Peterson, A. Potential for spread of the white-nose fungus (*Pseudogymnoascus destructans*) in the Americas. *Geospat Health*. **9**, 221–229. https://doi.org/10.4081/gh.2014.19 (2014).
51. Cobos, M. E., Townsend Peterson, A., Barve, N. & Osorio-Olvera, L. kuenm: An R package for detailed development of ecological niche models using Maxent. *PeerJ* **7**, e6281. https://doi.org/10.7717/peerj.6281 (2019).
52. Muscarella, R. et al. ENMeval: An R package for conducting spatially independent evaluations and estimating optimal model complexity for Maxent ecological niche models. *Methods Ecol. Evol.* **5**, 1198–1205. https://doi.org/10.1111/2041-210X.12261 (2014).

Figures

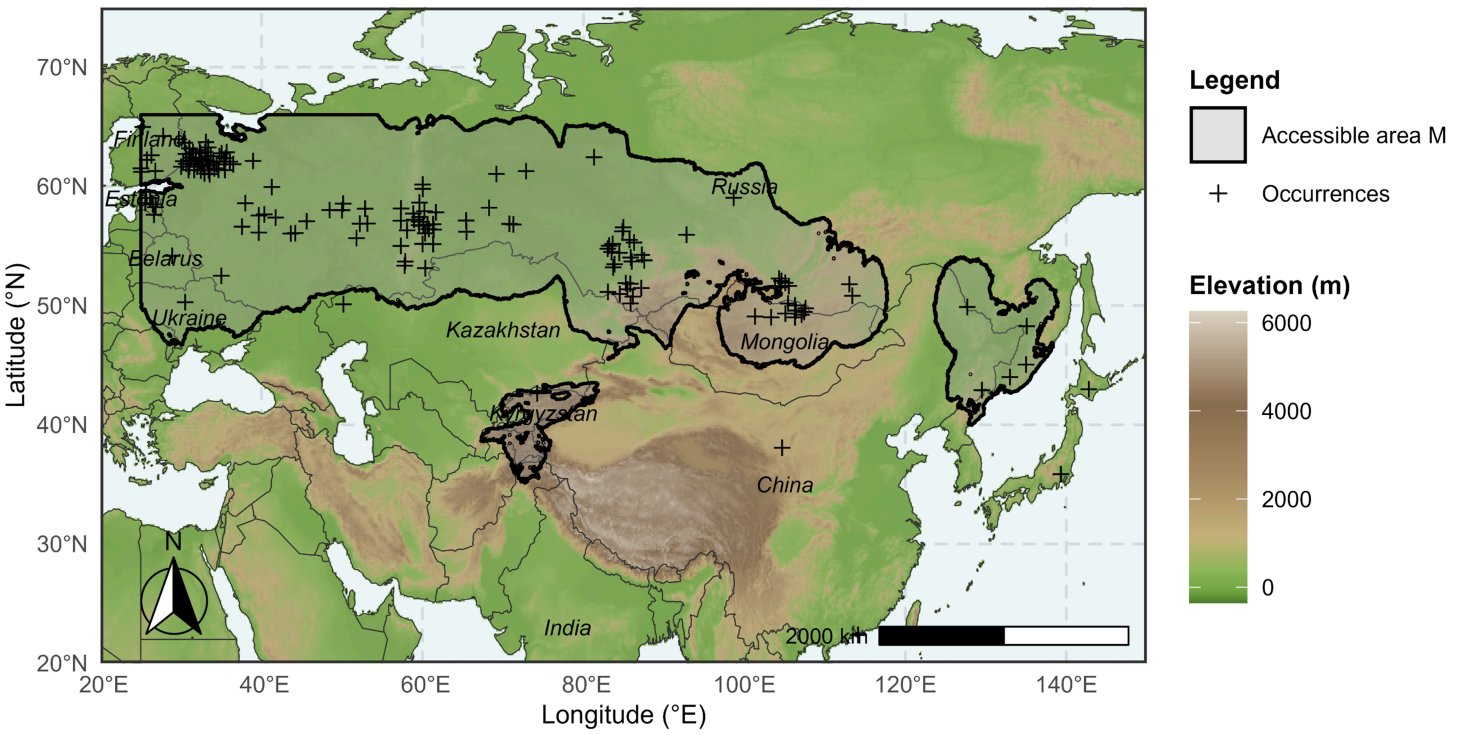


Figure 1

Occurrence locations of *Ixodes persulcatus* used for calibration of ecological niche models and the accessible area (M) defining the model calibration region. Points represent cleaned and spatially filtered occurrence records compiled from GBIF and Mongolian surveillance data. The shaded polygon indicates the estimated dispersal-accessible area used for model calibration.

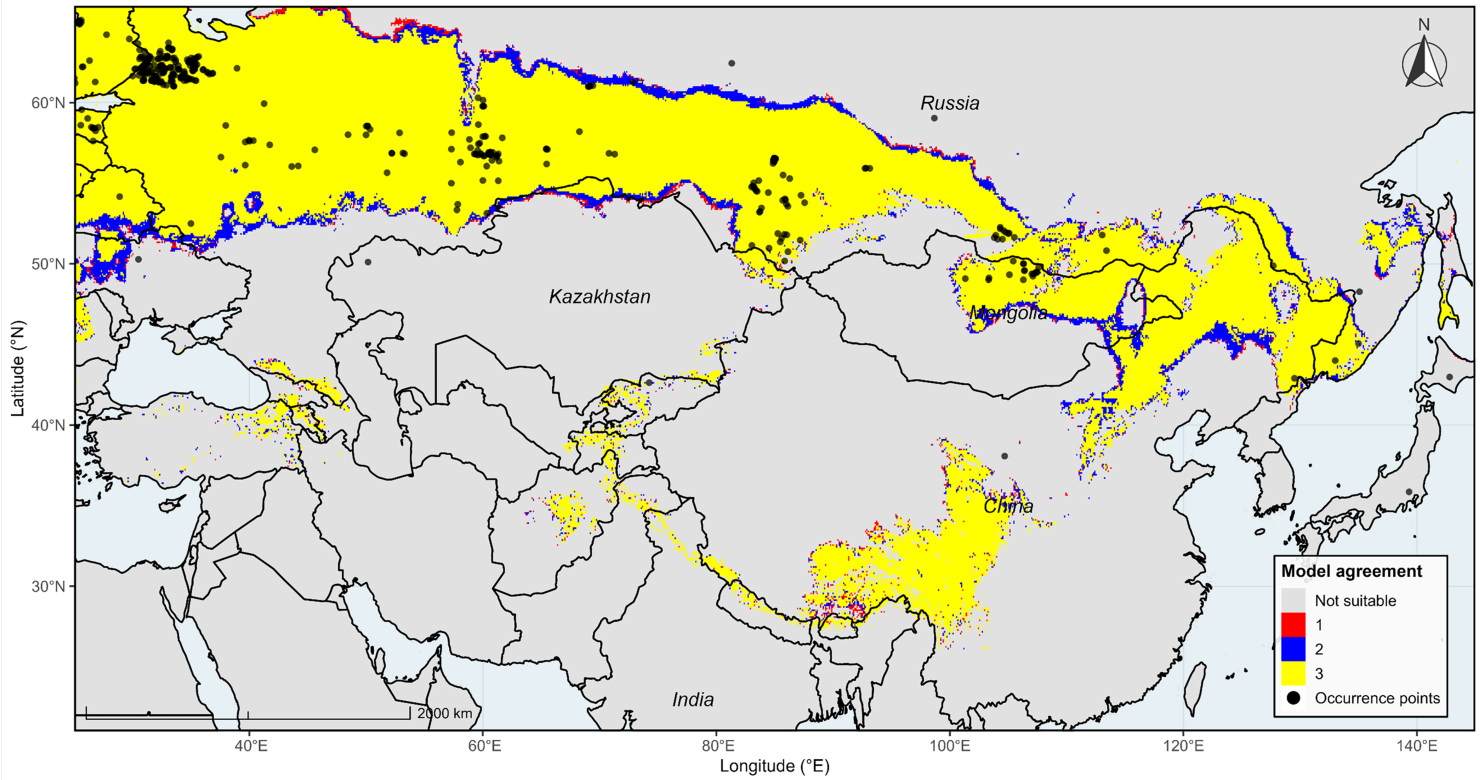


Figure 2

Predicted potential distribution of *Ixodes persulcatus* across Eurasia based on median ensemble agreement from best-fitting MaxEnt models. Colors represent the number of models predicting suitability in each pixel (1–3), yellow color indicate highest model agreement and greatest climatic suitability.

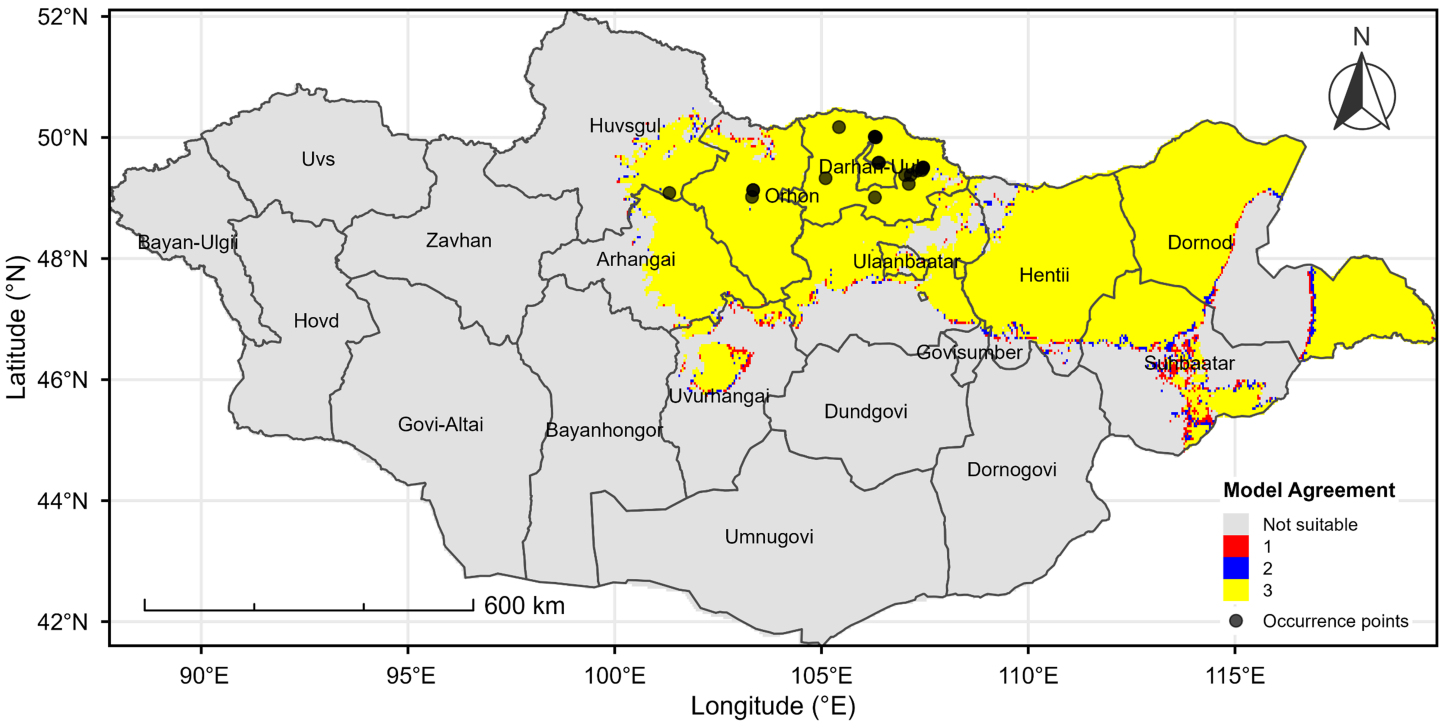


Figure 3

Predicted potential distribution of *Ixodes persulcatus* in Mongolia derived from median ensemble agreement of best-fitting MaxEnt models. Colors represent the number of models predicting suitability in each pixel (1–3),yellow color indicate highest agreement and highest climatic suitability. High-suitability regions are concentrated in northern, central, and northeastern Mongolia. Black dots represent occurrence records of *Ixodes persulcatus*.

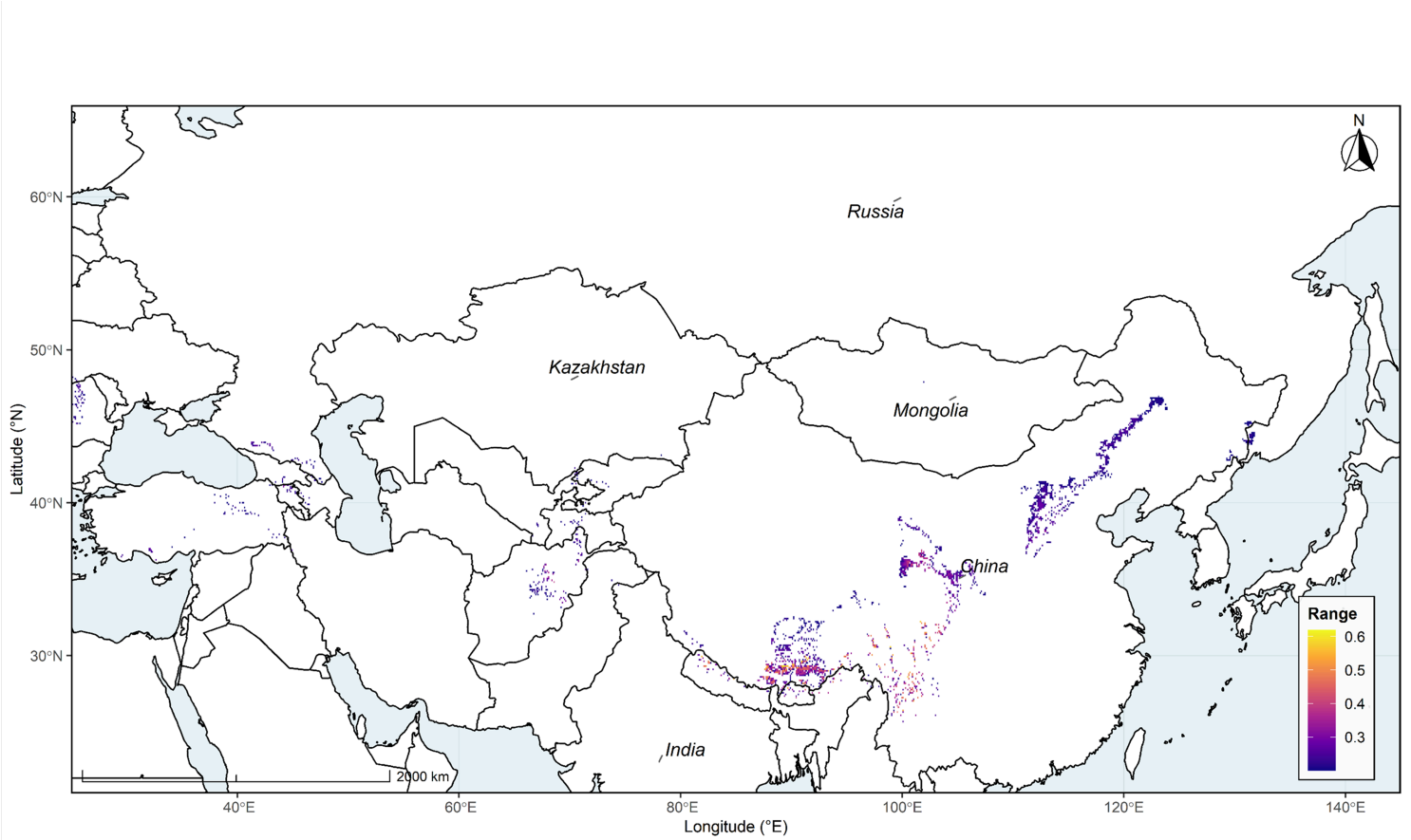


Figure 4

Uncertainty of predicted suitable areas of *Ixodes persulcatus* across Eurasia. Colors from purple to yellow indicate progressively higher uncertainty quantified as the pixel-wise range (maximum minus minimum) of predicted suitability values across models.

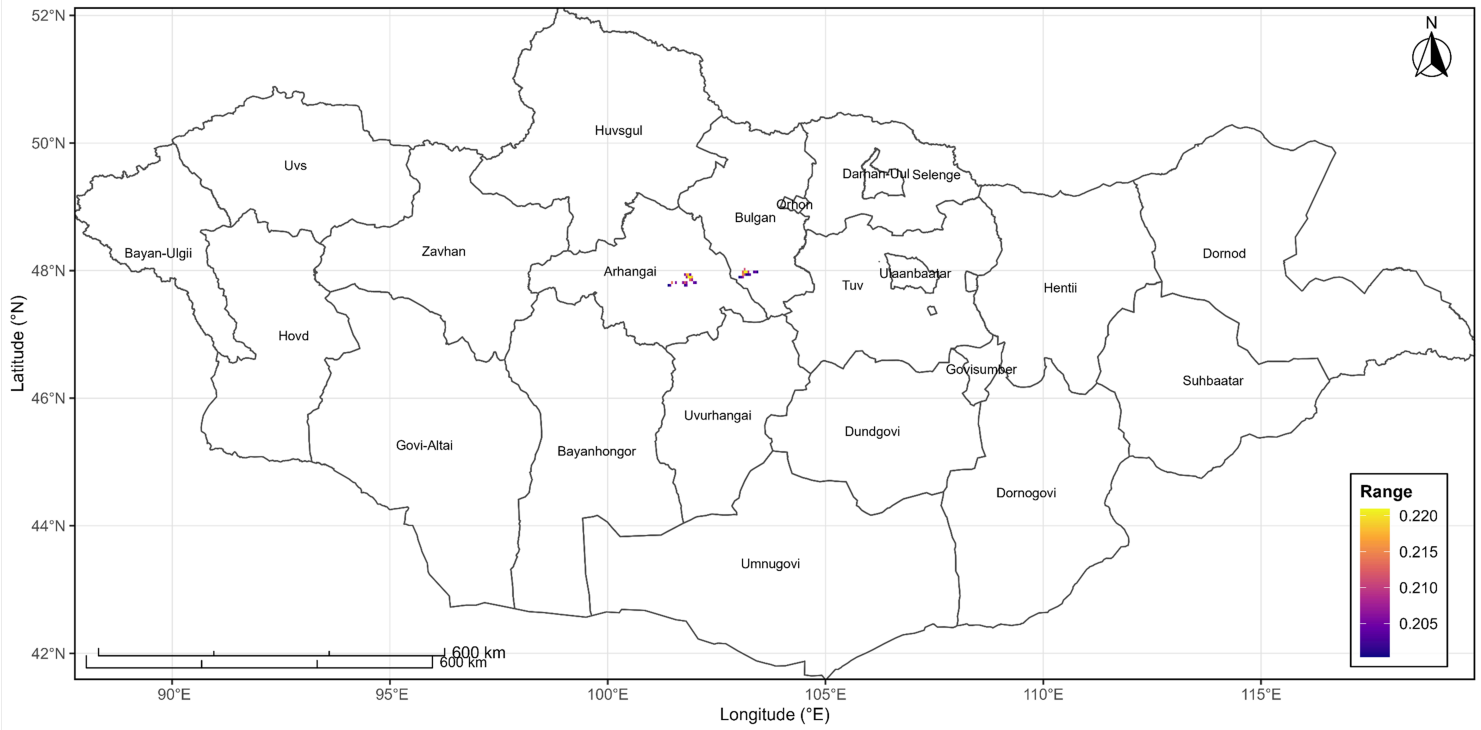


Figure 5

Uncertainty associated with the predicted suitable areas of *Ixodes persulcatus* in Mongolia. Colors from purple to yellow represent prediction uncertainty quantified as the pixel-wise range (maximum minus minimum) of predicted suitability across models. Areas with a range of ≤ 0.2 were considered to have low uncertainty.

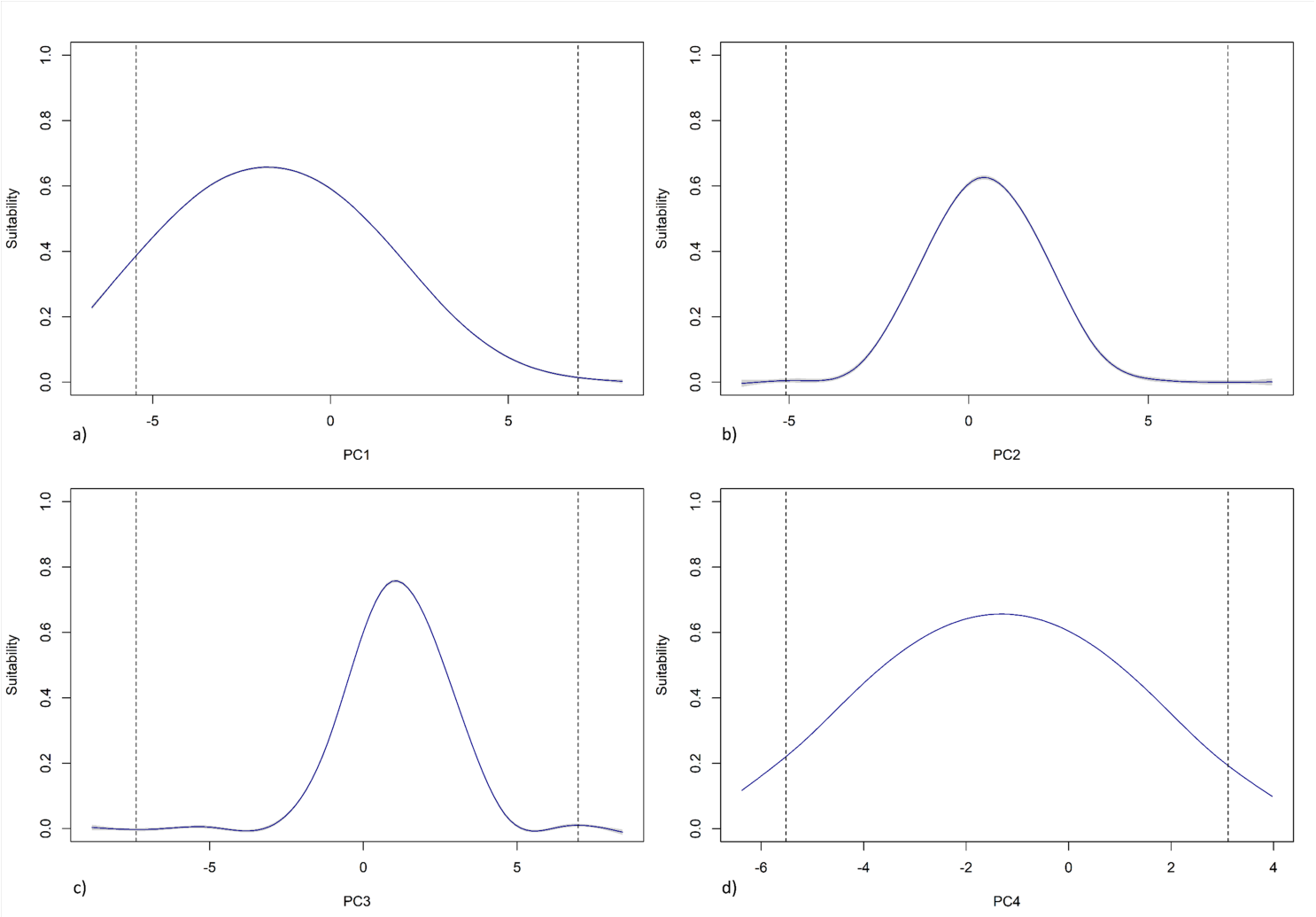


Figure 6

Model response curves for principal components (PC1–PC4) summarizing climatic predictors. Environmental variables were reduced using principal component analysis, and the first four components explaining 95% of total variance were retained. Curves depict marginal effects, showing how predicted suitability changes along each component while other predictors are held constant at their mean values. Dashed vertical lines indicate the range of PC values observed at occurrence locations. (a) PC1: suitability peaks at intermediate values reflecting cold-season severity and continentality. (b) PC2: unimodal response associated with warm-season temperature and wet-season precipitation. (c) PC3: narrow tolerance range linked to wet-season rainfall intensity. (d) PC4: broad unimodal response associated with temperature variability.

Supplementary Files

This is a list of supplementary files associated with this preprint. Click to download.

- Supplementaryinformation.docx